LOW-VELOCITY IMPACT LOCALIZATION OF THE COMPOSITE TUBE USING A NORMALIZED CROSS-CORRELATION METHOD

Hyunseok Kwon[1], Yurim Park[1], Pratik Shrestha[1] and Chun-Gon Kim[1*]

[1] Department of Aerospace Engineering, Korea Advanced Institute of Science and Technology, 291 Daehak-ro, Yuseong-gu, Daejeon, Republic of Korea
*E-mail: cgkim@kaist.edu, web page: http:/www.kaist.ac.kr

Keywords: Composite tube, Structural health monitoring, Impact localization, Fiber Bragg grating sensor

ABSTRACT

This study presents an experimental study on the low-velocity impact localization of cylindrical structures. A composite tube structure was used to represent cylindrical structures such as aircraft fuselage and tail boom. Three FBG sensors were used to acquire the impact signals, and the normalized cross correlation method was employed as the algorithm for localizing the random impact source. A total of 18 random impacts were applied to the composite tube using an impact hammer, and it was post-processed using the employed algorithm and reference database which was constructed in advance. When three sensors were used, the localization results were successfully estimated with the average error of 1.89cm and maximum error of 4.97cm. However, when two sensors were used, the results were negatively affected by the minimal distance between the sensors, so the results for the case using two sensors located farther apart showed lower average and maximum errors. Therefore, it shows that performance of the impact localization for the cylindrical composite structure is influenced by the number of sensors and the distance or configuration between the sensors.

1 INTRODUCTION

Since composite materials have high-specific strength and stiffness, it is being widely used in a variety of industrial fields, especially in the aerospace industry. Recently, the superiority of composite material was proved by the new Boeing 787 Dreamliner which is composed of more than 50% of composite materials. However, since composite materials have different damage types with regard to existing conventional metallic materials, Structural Health Monitoring (SHM) to check the state of composite structure during operation is essential for ensuring the safety and reliability. Among the damage types of composite materials, barely visible impact damage (BVID) caused by the low velocity impact such as tool drop, bird-strike could degrade the mechanical properties of a composite structure and finally lead to fatal accidents without perceiving beforehand. Therefore, to prevent the potential BVID, Various studies for low velocity impact localization have been conducted. However, the applicability of the previous studies is low because most of them adopted multiple electric sensors which offer several problems such as electro-magnetic interference (EMI) and wiring problems [2-4]. Since the fiber Bragg grating (FBG) sensor have excellent characteristics of small size, mutiplexability and EMI immunity, so it is being widely used in SHM research on composite structures to overcome the disadvantages of conventional electric sensors. Especially, since FBG sensor can easily be embedded into the composite materials with barely affecting mechanical properties of the composite materials, it is suitable for SHM of composite structure. In addition, the targeted structures of previous studies were concentrated to the wing box and the stiffened panel which cannot describe cylindrical structures such as the fuselage or tail boom [1, 4-5]. Lee et al [6] performed the impact localization on a aluminum pipe, but it needs to be applied to the cylindrical composite structures.

In this research, impact localization for composite tube based on FBG sensor using normalized cross-correlation was conducted. The composite tube which describe the cylindrical structure was targeted for impact localization, and a FBG sensor which have excellent characteristics was selected.

2 EXPERIMENTAL SETUP

As a target structure, a composite tube which describes the cylindrical structures of an aircraft such as tail boom and fuselage was selected. The composite tube was fabricated using a carbon/epoxy Prepreg (CU125NS, SK Chemical Co., Republic of Korea). The stacking sequence of the composite tube is $[0/\pm45/90]_s$, and the composite tube has a diameter of 100mm and a length of 300mm. Figure 1 shows the fabricated composite tube.

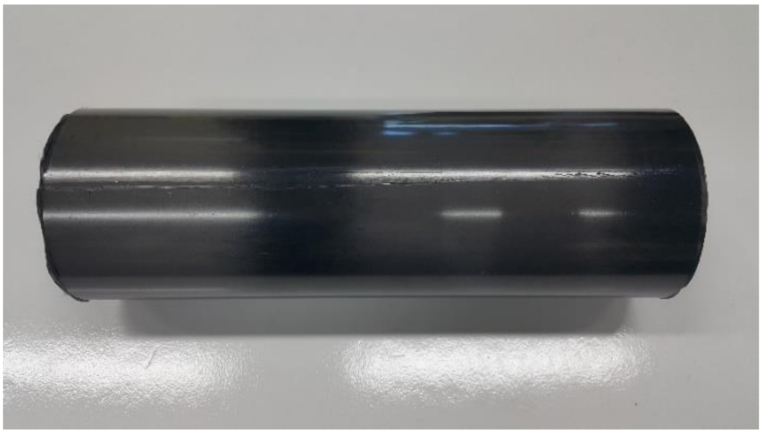

Figure 1: Fabricated composite tube.

One end of the composite tube structure was clamped to a fixture, as shown in figure 2. The test section for the impact localization was 150 (longitudinal direction) × 200 (circumferential direction), and it was 90mm away from the clamped boundary. The test section consists of 63 grid points, and the distance between parallel or perpendicular grid points was 25mm. FBG sensors (FBG KOREA, Inc., Rep. of Korea) which have a center wavelength of 1544.7nm, 1550.4nm, 1553.6nm and a gauge length of 10mm were chosen. The FBG sensors were attached to the surface of the specimen using the same procedure of a strain gauge. The intervals of each FBG sensor were 50mm in the circumference direction, and it was attached at an angle of 45 degrees to the centerline. The attached FBG sensors were connected to a commercial high-speed interrogator (Fiberpro, Inc., Rep. of Korea). The impact signals were acquired with a sampling frequency of 100kHz, the data length of the signals was 4500. Figure 2 shows the experimental setup.

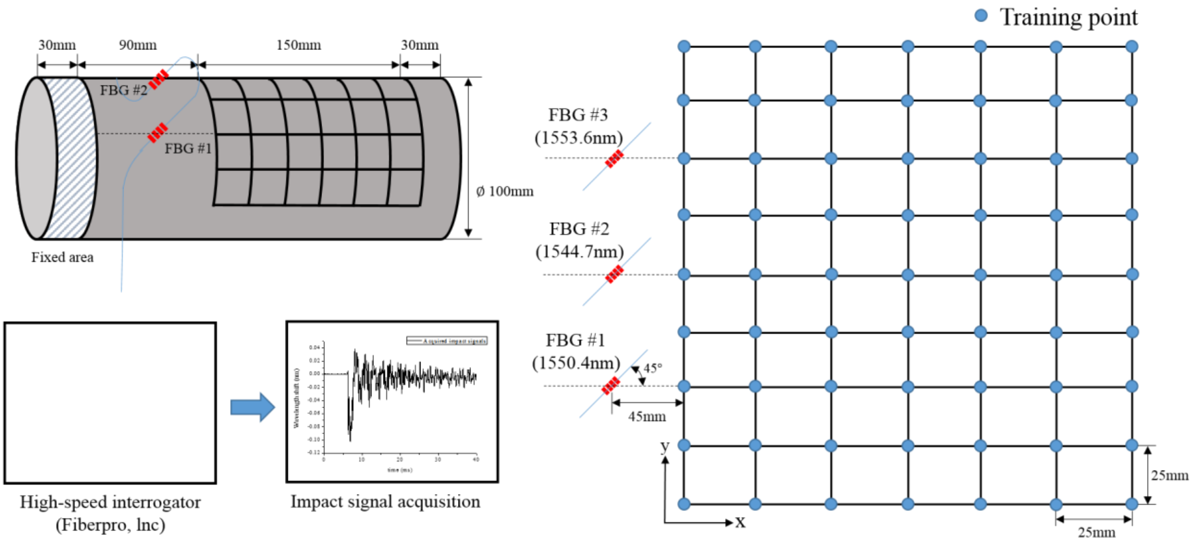

Figure 2: Experimental setup.

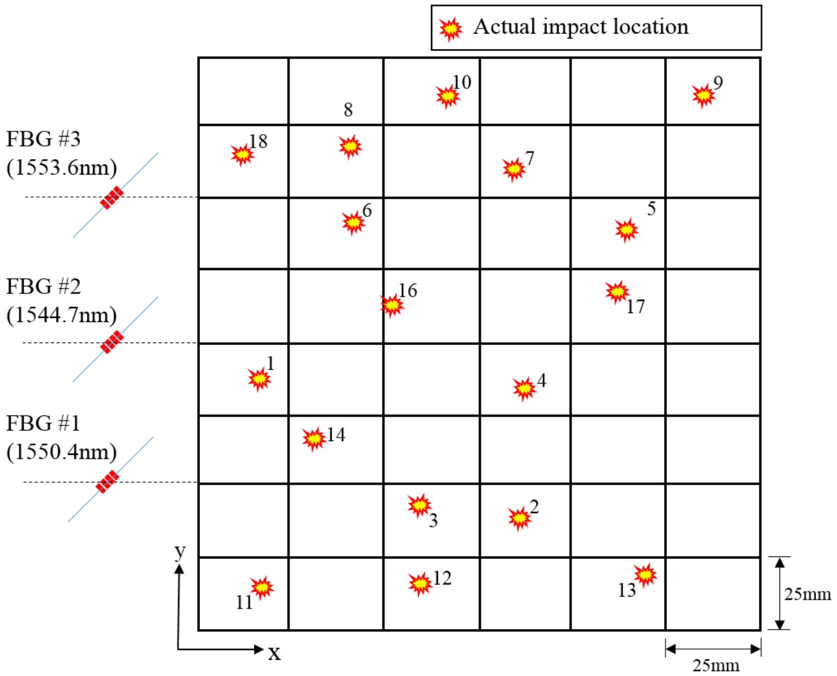

Impact point	x (mm)	y (mm)
1	1.6	8.7
2	8.6	3.7
3	6.0	4.4
4	8.7	8.3
5	11.6	13.7
6	4.1	14.1
7	8.6	16.0
8	4.0	17.1
9	13.4	18.4
10	6.8	18.5
11	1.6	1.4
12	5.9	1.6
13	11.8	1.8
14	3.2	6.6
15	11.9	5.7
16	5.2	11.2
17	11.1	11.9
18	1.3	16.5

Figure 3: locations of 20 impact points.

As shown in figure 3, a total of 18 random impacts were applied using the impact hammer.

3 IMPACT LOCALIZATION ALGORITHM

Figure 3 shows the flow chart of the employed algorithm proposed by Kim [1]. The employed algorithm is divided into two sections. The first part is to extract the proper signal form from the acquired signals for proper comparison between different signals. In this process, the obtained signals is adjusted to the baseline and signal is cut off using arrival time of the signal. The second part is to estimate the actual impact location using normalized cross-correlation method. The normalized cross-correlation method is based on cross-correlation method. The cross-correlation method is used to calculate and compare the similarity between two different signals. When the similarity between two signals is high, it shows a high value and in the opposite case it shows a low value. Therefore, the actual impact locations is estimated using the reference signal at each grid point that is constructed in advance. The cross-correlation between two signals is as shown below.

$$(\mathrm{f} * \mathrm{g})(\tau) = \int_{-\infty}^{\infty} f(t)g(t+\tau)dt \tag{1}$$

In equation (1), * is the cross-correlation operator, and τ is the time-lag between the two different signals f and g . The normalized cross-correlation modified the existing cross-correlation using by adding the normalization procedure. The employed normalized cross-correlation is shown below.

$$\left(\frac{f}{F} * \frac{g}{G}\right)(\tau) = \frac{1}{F(kF)}(f * kf)(\tau) = \frac{1}{F^2}(f * f)(\tau) \tag{2}$$

In equation (2), F and G are the normalizing constant, and k is a constant between the two impact signals for an ideal case. It has been proved that the performance of the normalized cross correlation is better than cross correlation method by Kim [1]. The similarity between the random impact signal and the reference signals at each grid point is calculated using the normalized cross correlation, and for all grid points exceeding a correlation value of 90% of maximum, the centroid among them is predicted to be the actual impact location.

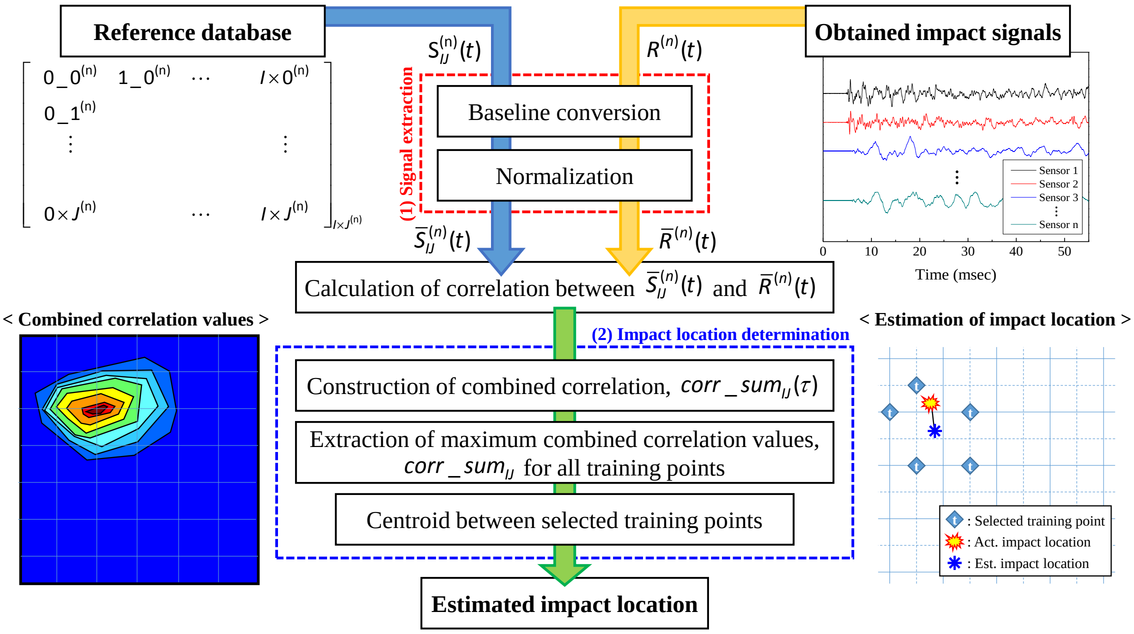

Figure 4: Flow chart for the impact localization algorithm by Kim [1].

4 RESULTS

Figure 5 shows the impact localization results based on three FBG sensors using the employed normalized cross-correlation algorithm. The average error was 1.89mm with a standard deviation of 1.16mm, and the maximum error was 4.97mm. The average error and standard deviation were similar to the results of impact localization for aluminum pipe structure based on the FBG sensor using root means squired value-based algorithm by Lee [6]. However, if less than 3 sensors were used, the results were different.

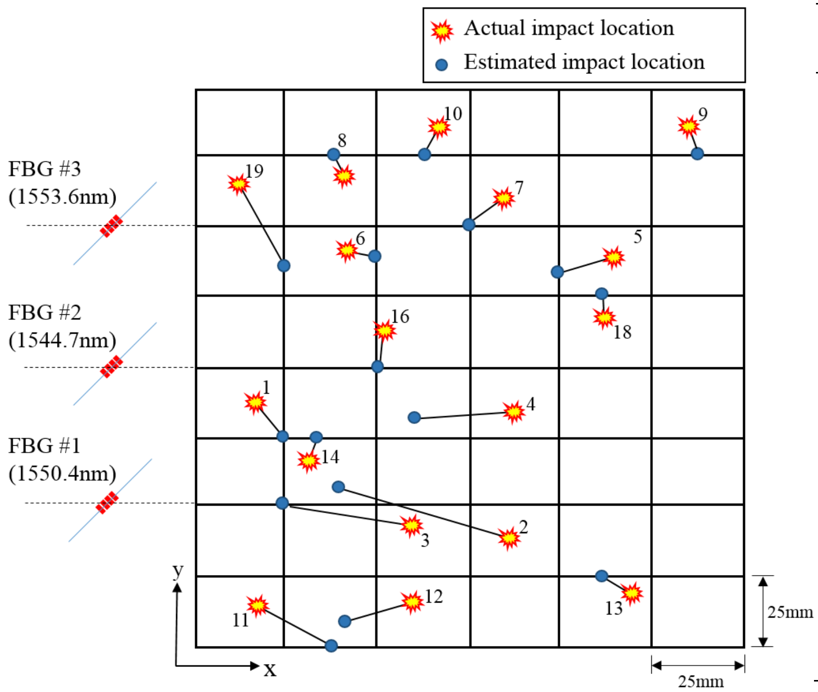

Estimated point	x (mm)	y (mm)
1	25.0	75.0
2	39.5	54.7
3	25.3	50.0
4	60.3	82.9
5	99.8	131.0
6	50.0	138.4
7	75.0	150.0
8	36.9	175.0
9	137.72	175.0
10	50.0	175.0
11	36.8	0.0
12	41.27	8.23
13	113.0	25.0
14	35.0	75
15	50.0	100.0
16	86.6	150.0
17	112.4	125.0
18	24.1	135.32

Figure 5: Estimated impact locations using three FBG sensors.

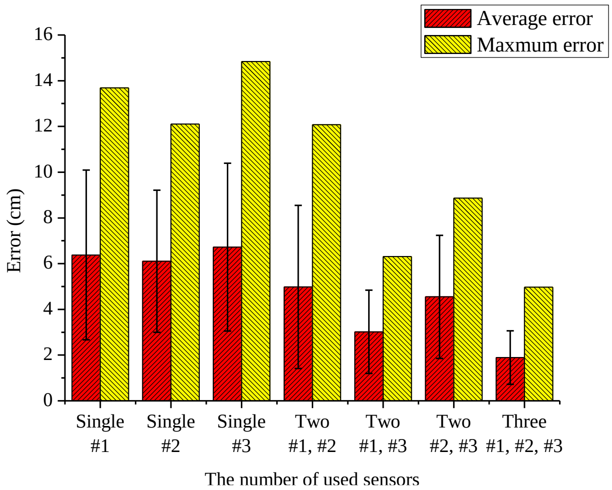

Figure 6: The error of the estimated impact locations according to the number of FBG sensors.

Figure 6 shows the impact localization results according to the number of FBG sensors. In the case of using a single FBG sensor, average error of more than 6cm and maximum error of more than 12cm were shown. If two sensors were used, the results were different depending on whether or not they included FBG # 2 sensors installed in the center line of the test section. When the two FBG sensors including FBG # 2 sensor were used, it showed an average error of more than 4.5cm with high standard deviation and a maximum error of approximately 9cm. However, when FBG # 2 sensor was not used, the average error was approximately 3 cm with less standard deviation and maximum error was less than 7 cm. This is a result of a 36% reduction in the average error compared to the results using #2 FBG sensor. The FBG # 2 sensor was installed in the center line, but it is expected to be not a because it was installed at an angle of 45 degrees to avoid symmetrical signal acquisition in the upper and lower areas with respect to the center line. Figure 7 shows the comparison of the acquired impact signals at the difference points which are symmetrically located with regard to centerline at the test section. The acquired signals at the symmetrical points shows the low similarity, so it can be confirmed that FBG #2 sensor don't have any signal similarity with regard to the center line.

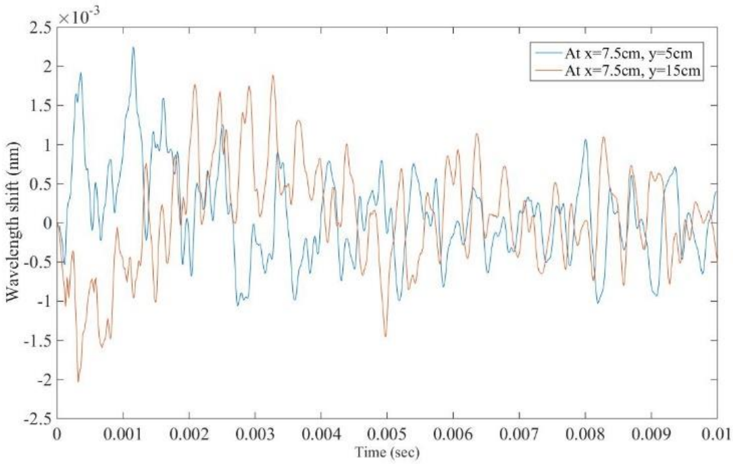

Figure 7: The comparison of acquired impact signals at symmetrical grid points.

The reason for reduction of error might be because the interval between the sensors is wider. Hence, the cross-correlation value can be compensated with each other as compared with the case where the intervals between the sensors are close to each other. In the case of previous research, the distance between the sensors were 50mm and 100mm. However, since the diameter of the pipe was 60.7mm, the relative distance between the sensors was wider than this experiment and thus shows better results.

Therefore, it might be better to use many sensors to improve the impact localization performance of a cylindrical structure, or to not install the sensor in close proximity to another sensor.

5 CONCLUSIONS

In this study, low-speed impact localization was conducted on the composite tube which represent cylindrical structures. Three FBG sensors were used to acquire the impact signals, and a normalized cross correlation method was employed as the algorithm for localizing the random impact source. A total of 18 random impacts was applied to the composite tube using the impact hammer, and it was post-processed using the employed algorithm. When three sensors were used, the average error and the standard deviation were similar to those of the impact localization for aluminum pipe structure by previous research. However, if less than 3 sensors were used, the results were negatively affected by the nominal distance between sensors. Especially, the accuracy was decreased when the sensors located close to each other were used. Since the configuration of FBG sensors in the study by previous research was relatively wider compared to diameter of the aluminum pipe, the results can be contributed to the close arrangement of sensors. Therefore, it would be better to use many sensors to improve the impact localization performance of the cylindrical structure, or to not install the sensor in close proximity. Furthermore, further work for various sensor location is needed to determine the effective location for sensors in the cylindrical structures because the sensors used in this study were concentrated on the upper surface.

ACKNOWLEDGEMENTS

This research was supported by the Technology Innovation Program funded by the Ministry of Trade, Industry & Energy (MI, Korea) (10047457, Development of aircraft health monitoring integrated measurement system for composite.

REFERENCES

[1] J.-H. Kim, Y.-Y. Kim, Y Park and C.-G. Kim, Low-velocity impact localization in a stiffened composite panel using a normalized cross-correlation method, *Smart Materials and Structures*, **24(4)**, 2015, pp. 45036 (doi: 10.1088/0964-1726/24/4/045036).

[2] R.K. Ing, N. Quieffin, S. Catheline and M. Fink, In solid localization of finger impacts using acoustic time-reversal process, *Applied Physics Letter*, **87(20)**, 2005, pp. 2004104 (doi: 10.1063/1.2130720).

[3] F. Ciampa and M. Meo, Impact localization on a composite tail rotor blade using an inverse filtering approach, *Journal of Intelligent Material Systems and Structures,* **25(10)**, 2014, pp. 1950-1958 (doi: 10.1177/1045389X13512904).

[4] B. Park, H. Sohn, S.E. Olson, M.P. DeSimo, K.S. Brown and M.M. Derriso, Impact localization in complex structures using laser-based time reversal, *Structural Healt Monitoring*, **11(5)**, 2012, pp. 577-588 (doi: 10.11177/1475921712449508).

[5] B.-W. Jang, Y.-G. Lee, J.H. Kim, Y.Y. Kim, C.-G. Kim, Real-time impact identification algorithm for composite structures using fiber Bragg grating sensors, *Structural Control and Health Monitoring*, **19**, 2012, pp. 580-591 (doi: 10.1002/stc.1492).

[6] Y.-G. Lee and C.-G. Kim, Impact source identification for pipe structure based on a one-dimensional fiber Bragg grating sensor array, *Journal of Intelligent Material Systems and STructures*, **69**, 2016, pp. 228-238 (doi: 10.1177/1045389X16679292).